



BELLE2-NOTE-PL-2020-XXX
Draft version 1.0
July 31, 2020

Muon and electron identification efficiencies and hadron-lepton mis-identification probabilities

The Belle II Collaboration

Abstract

In this note we show the performance of Belle II electron and muon identification, based on a combination of subdetector likelihoods. The studies are carried out using the Belle II collision data of 2019 and early 2020. The analysed on-resonance dataset corresponds to an integrated luminosity of $\int L dt = 34.6 \text{ fb}^{-1}$, with an additional $\int L dt = 3.2 \text{ fb}^{-1}$ of off-resonance data taken during 2020.

1. DATASET AND DEFINITIONS

The lepton identification studies ($\ell^\pm = \{e^\pm, \mu^\pm\}$) presented in this document have been performed using the ICHEP on-resonance datasets from 2019 (experiments 7, 8 and 10) 8.8 fb^{-1} , and 2020 (experiment 12) 25.8 fb^{-1} , as well as the 2020 off-resonance dataset for the D^{*+} channel (experiment 12) 3.2 fb^{-1} .

Information from each particle identification system (CDC, TOP, ARICH, ECL, KLM) is analysed independently to determine a likelihood for each charged particle hypothesis. These likelihoods may then be used to construct a combined likelihood ratio. In the plots presented here we study identification based on the global likelihood ratio (from all the subdetectors) defined as:

$$\ell\text{ID} = \frac{\mathcal{L}_\ell}{\mathcal{L}_e + \mathcal{L}_\mu + \mathcal{L}_\pi + \mathcal{L}_K + \mathcal{L}_p}. \quad (1)$$

We report the lepton identification performance of electron-hadron, and muon-hadron separation ($h^\pm = \{\pi^\pm, K^\pm\}$) using a complementary set of decay channels. Electron and muon identification efficiencies are studied using $e^+e^- \rightarrow \ell^+\ell^-(\gamma)$, $e^+e^- \rightarrow e^+e^-\ell^+\ell^-$, and $J/\psi \rightarrow \ell^+\ell^-$, while pion mis-identification rates are studied using $K_S^0 \rightarrow \pi^+\pi^-$, $e^+e^- \rightarrow \tau^\pm(1P)\tau^\mp(3P)$, and $D^{*+} \rightarrow D^0(\rightarrow K^-\pi^+)\pi^+$. The latter is also used to determine kaon misidentification rates. Efficiencies and misidentification rates are defined as follows:

$$\epsilon(\ell) = \frac{\text{number of electron (muon) tracks identified as an electron (muon)}}{\text{total number of electron (muon) tracks}}, \quad (2)$$

$$\text{mis-ID rate}(h \rightarrow \ell) = \frac{\text{number of charged hadron tracks identified as an electron (muon)}}{\text{total number of charged hadron tracks}} \quad (3)$$

Other techniques for combining subdetector data, such as a boosted decision tree methods, have also been developed for Belle II but are not yet used for physics analysis studies and therefore not covered here.

Performance is evaluated in the polar angle acceptance regions corresponding to the electromagnetic calorimeter (ECL) for electrons (0.22 to 2.71 radians), and to the K_L^0 -muon detector (KLM) for muons (0.40 to 2.60 radians). Combined, the set of probe channels covers a lab-frame momentum range of $0.4 \text{ GeV}/c$ to $7.0 \text{ GeV}/c$. For efficiencies, results are also binned with respect to their lab frame polar angle and measured track charge (the latter are not shown here).

Lepton identification performance is studied for three reference selection thresholds on the ℓID variable: 0.5, 0.9 and 0.95. For brevity, the plots hereby presented show results for a selection of $\ell\text{ID} > 0.9$.

2. RESULTS

Signal reconstruction plots from lepton efficiency studies are shown for $J/\psi \rightarrow \ell^+\ell^-$ (Fig. 1), $e^+e^- \rightarrow e^+e^-\ell^+\ell^-$ (Fig. 2), $e^+e^- \rightarrow \mu^+\mu^-\gamma$ (Fig. 3), and $e^+e^- \rightarrow e^+e^-(\gamma)$ (Fig. 4). Signal reconstruction plots from misidentification rate studies are shown for $K_S^0 \rightarrow \pi^+\pi^-$ (Fig. 5), $D^{*+} \rightarrow D^0(K^-\pi^+)\pi^+$ (Fig. 6), and $e^+e^- \rightarrow \tau^\pm(1P)\tau^\mp(3P)$ (Fig. 7).

We overlay the efficiency and misidentification rates for two hadronic channels, J/ψ and K_S^0 for `electronID` > 0.9 integrated over the ECL barrel region (Fig. 8) and `muonID` > 0.9 integrated over the KLM barrel region (Fig. 9). In these regions, the average identification efficiency is $\approx 94\%$ (electrons), $\approx 90\%$ (muons), for a pion misidentification rate of $\approx 2\%$ (electrons) $\approx 4\%$ (muons), respectively. Finally we overlay efficiencies and misidentification rates for all channels in two example barrel region polar angle bins for `electronID` (Fig. 10) and `muonID` for the same selection cut (Fig. 11).

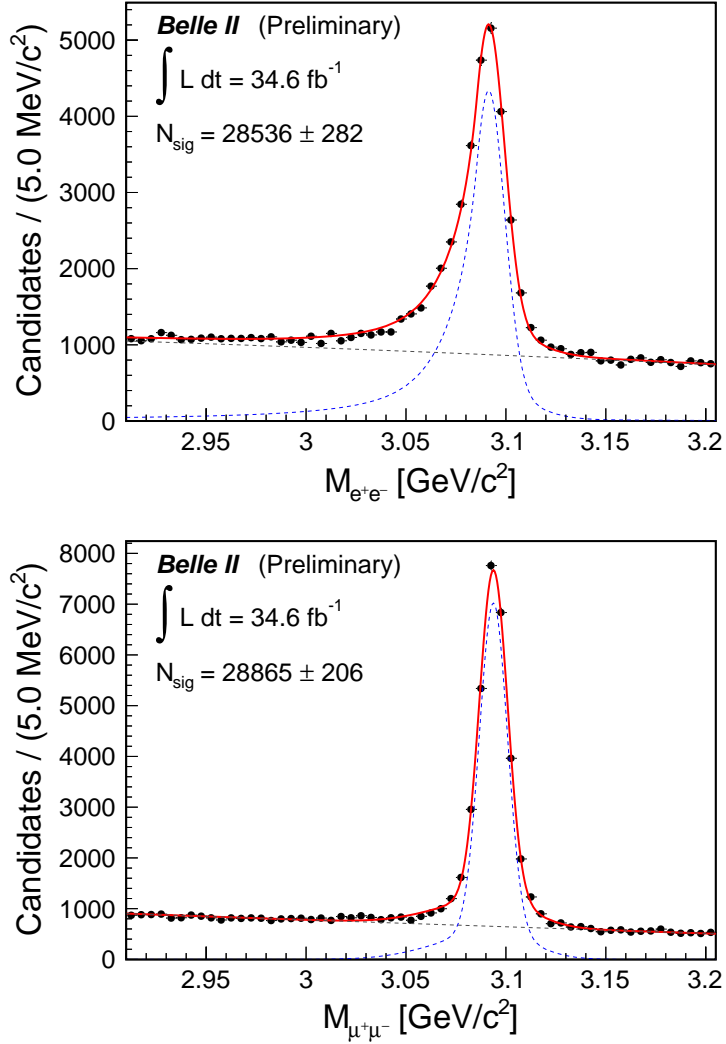


FIG. 1: The dielectron invariant mass of $J/\psi \rightarrow e^+e^-$ candidates (top), and dimuon invariant mass of $J/\psi \rightarrow \mu^+\mu^-$ candidates (bottom). The selection criteria for each candidate are as follows: $|dr| < 2.0$ cm, $|dz| < 5.0$ cm, $p_{\text{lab}} > 0.1$ GeV/ c and $\text{electronID} > 0.9$ or $\text{muonID} > 0.9$ for each track. A vertex fit using `KFit` was applied, selecting candidates that did not fail the fit. A bremsstrahlung correction was applied to electron candidates, which adds the 4-vectors of nearby photons to the electron 4-vector. For the electron channel, the signal is modelled by a Crystal Ball function summed with a bifurcated Gaussian and a Gaussian. For the muon channel, a Gaussian function summed with a bifurcated Gaussian is used. A second order polynomial is used to model the background for both channels. The width of an invariant mass distribution is measured by finding 68% coverage, denoted as σ_{68} , taken from the difference in mass between the 16% and 84% percentile of the signal fit, and then dividing by 2. The dielectron sample is found to have a width of about 0.024 GeV/ c^2 , while the dimuon sample has a width of 0.009 GeV/ c^2 .

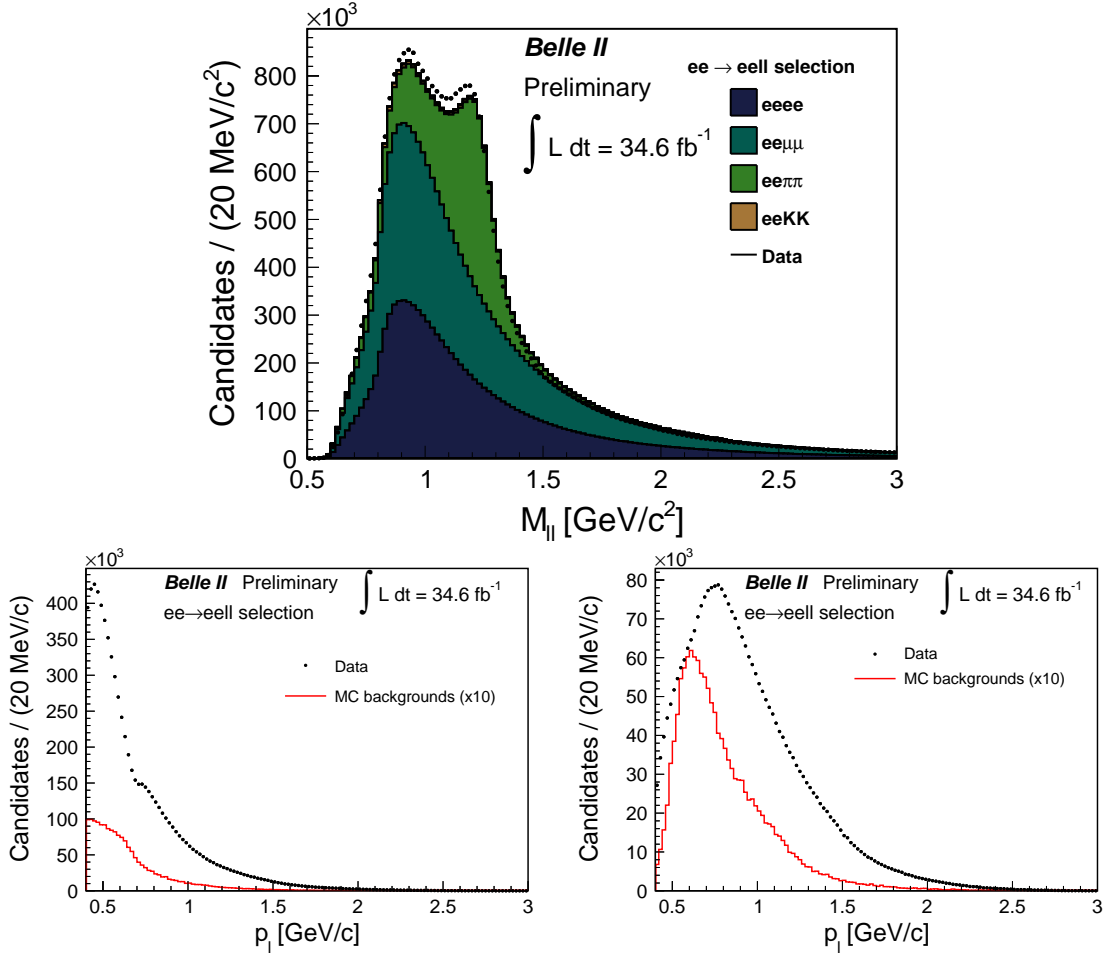


FIG. 2: Top row: the dilepton invariant mass in $e^+e^- \rightarrow e^+e^-\ell^+\ell^-$. The selection criteria for each track are as follows: $|dr| < 2.0 \text{ cm}$, $|dz| < 5.0 \text{ cm}$, $p_{\text{lab}} > 0.4 \text{ GeV}/c$. Tag selection criteria are not applied in this figure. The dilepton invariant mass is required to be less than $3 \text{ GeV}/c^2$ and the event is required to have a visible energy in the CMS frame of $E_{\text{vis}} < 6 \text{ GeV}$. Bottom row: the electron (left) and muon (right) lab-frame momentum distributions. In these plots, a tag selection of > 0.9 is applied. The red histogram (scaled up by a factor 10 for illustrative purposes) shows the overall background contamination, which amounts to $\approx 2.3\%$ ($\approx 4.9\%$) in the electron (muon) case. In both cases, most of the background is from the $e^+e^- \rightarrow e^+e^-\pi^+\pi^-$ process.

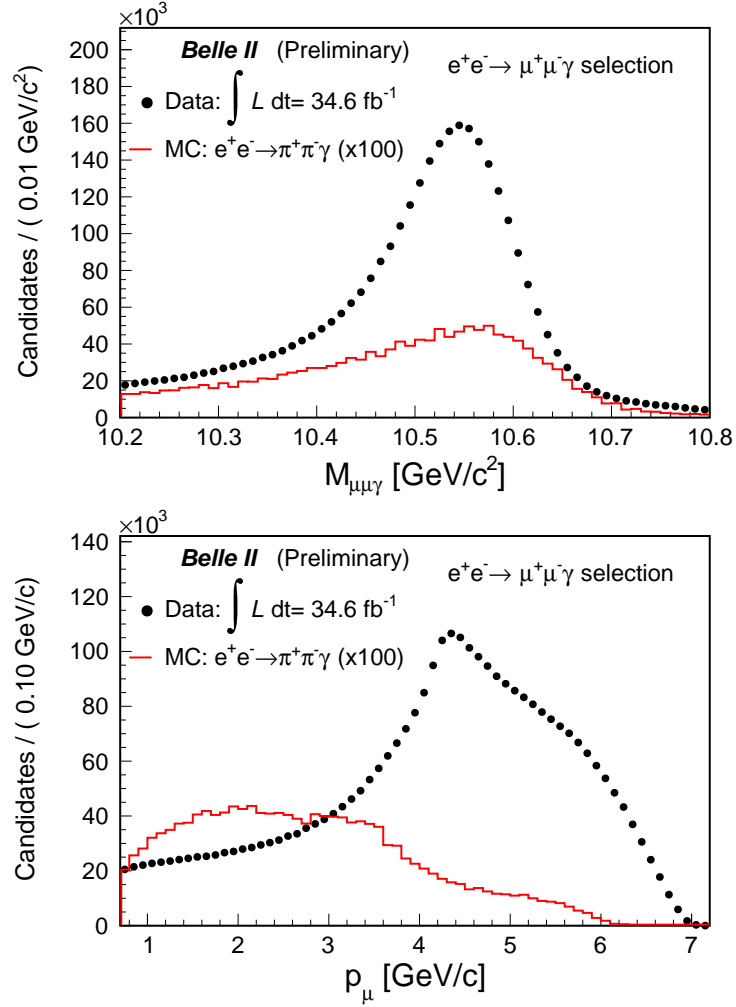


FIG. 3: The dimuon invariant mass (top), and muon lab-frame momentum (bottom) in $e^+e^- \rightarrow \mu^+\mu^-\gamma$. The selection criteria for each track are as follows: $|dr| < 2.0$ cm, $|dz| < 5.0$ cm, $p_{\text{lab}} > 0.7$ GeV/c with a tag requirement of $\text{muonID} > 0.9$. The event must contain only 2 tracks. The radiated photon must have an energy $E > 0.2$ GeV . The invariant mass of the the $\mu\mu\gamma$ system is required to be in the range $10.2 \text{ GeV} < M_{\mu\mu\gamma} < 10.8 \text{ GeV}/c^2$. Background from misidentified hadrons (electrons) are estimated to be less than 1% (0.1%).

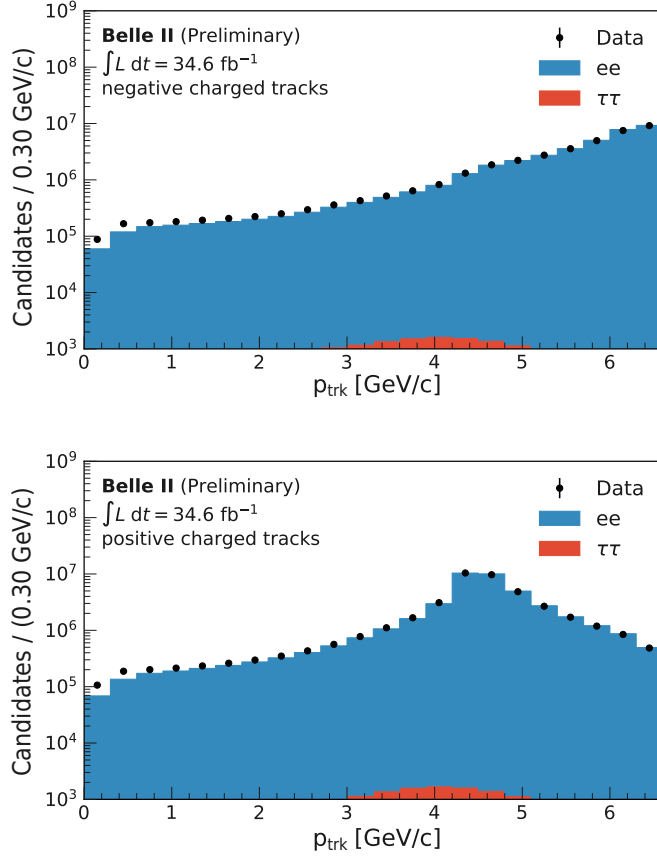


FIG. 4: The electron momentum (top), and positron momentum (bottom) in $e^+e^- \rightarrow e^+e^-(\gamma)$. The selection criteria for each track are as follows: $|dr| < 2.0$ cm, $|dz| < 5.0$ cm. A selection on the squared invariant mass of the system recoiling against the reconstructed e^+e^- pair of $M_{recoil}^2 < 10$ GeV^2/c^4 is applied to suppress hadronic background. The event must contain only 2 tracks and be triggered by an ECL cluster based low-multiplicity trigger (lml1). The tag track must have an energy of at least $E > 2$ GeV to minimise trigger bias.

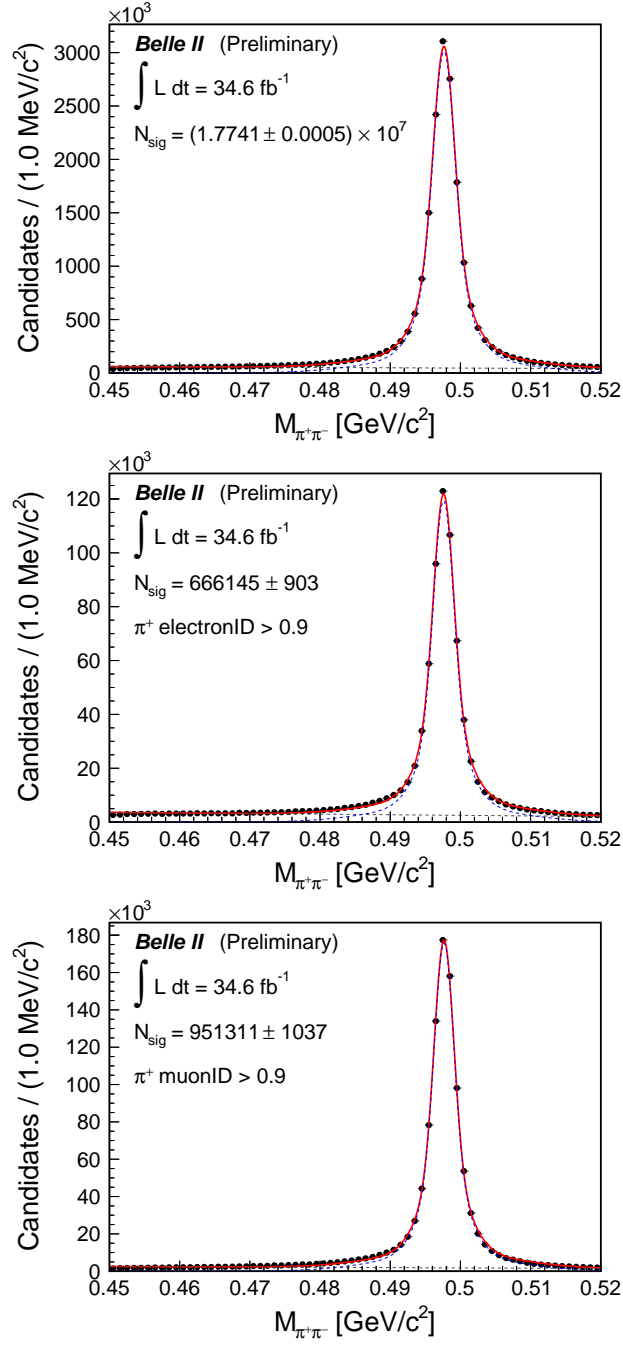


FIG. 5: The dipion invariant mass of $K_S^0 \rightarrow \pi^+ \pi^-$ before (top) and after application of $\text{electronID} > 0.9$ (middle) and $\text{muonID} > 0.9$ (bottom) on one track. The selection criteria for each track are as follows: $|dr| < 2.0 \text{ cm}$, $|dz| < 5.0 \text{ cm}$, $p_{\text{lab}} > 0.1 \text{ GeV}/c$. A vertex fit using *KFit* was applied, selecting candidates that do not fail the fit. The cosine of the angle between the K_S^0 momentum vector and the decay vertex position vector is required to be $\cos(\theta(\vec{p}_{K_S^0}, \vec{V}_{K_S^0})) > 0.998$. A triple Gaussian is used to model the signal and a first order polynomial is used to model the background.

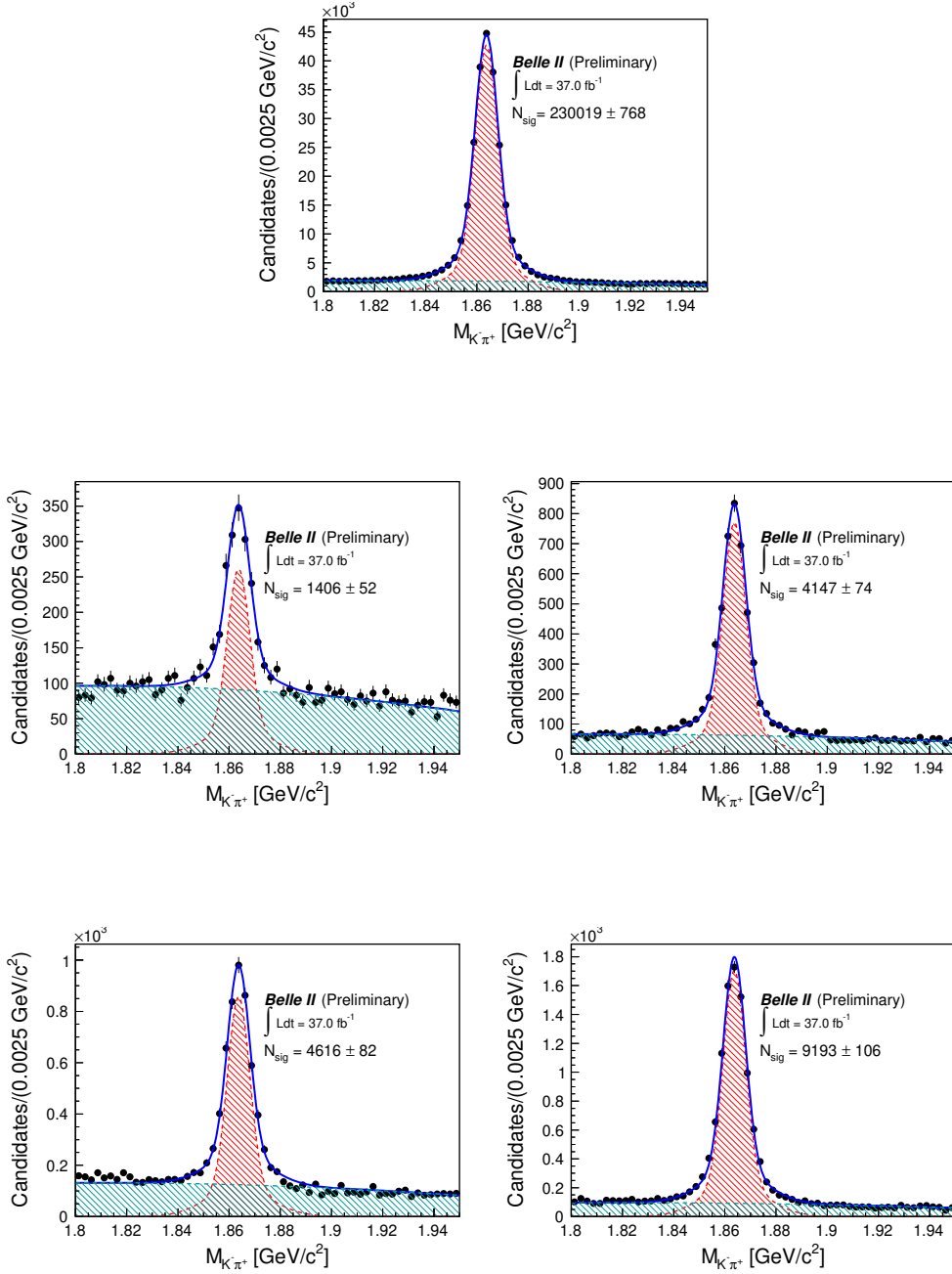


FIG. 6: $D^{*+} \rightarrow D^0(\rightarrow K^-\pi^+)\pi^+$ invariant mass plots without probe selection criteria (top), with $\text{electronID} > 0.9$ for the kaon track (middle left), with $\text{muonID} > 0.9$ for the kaon track (middle right), with $\text{electronID} > 0.9$ for the pion track (bottom left), and with $\text{muonID} > 0.9$ for the pion track (bottom right). The selection criteria for each track are as follows: $|dr| < 2.0$ cm and $|dz| < 4.0$ cm. The momentum of the D^{*+} in the CMS frame ($p_{D^{*+}}$) is required to be $> 2.5\text{GeV}/c$ to select prompt charm. A mass window on the $D^0 - D^{*+}$ mass difference $|\Delta M - 0.1453| < 1.5\text{MeV}/c^2$ is required. A double Gaussian signal function with a common mean is used to model the signal and a second order polynomial is used to model the background. The integrated luminosity of the dataset considered for this study corresponds to the combination of both on- and off-resonance data.

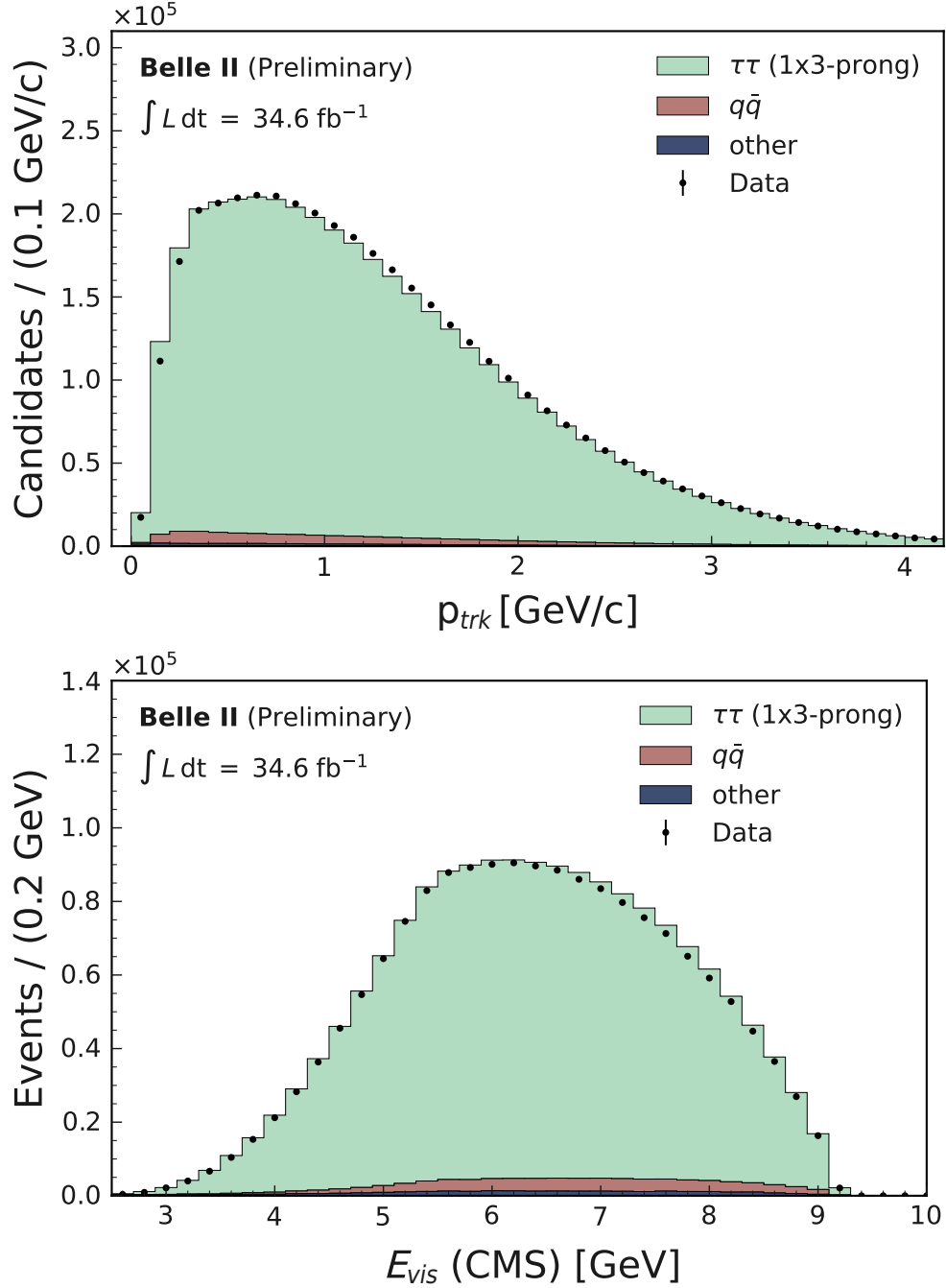


FIG. 7: The momentum of all tracks from the 3-prong decay (3P) $\tau \rightarrow h^+h^-h^+(nh^0)\nu$ (top), and visible event energy in the CMS frame in $e^+e^- \rightarrow \tau(1P)\tau(3P)$ events (bottom). The selection criteria for each track on the 1P and 3P sides are as follows: $|dr| < 1.0 \text{ cm}$, $|dz| < 3.0 \text{ cm}$. The track on the 1P side is required to have $p_{lab} > 0.1 \text{ GeV}/c$. Three charged tracks are required to be in one hemisphere (3P-candidates) while only one is in the other (1P candidate). TreeFitter is used to perform a vertex fit on the 3-prong side and a requirement on the p -value is employed to suppress combinatorial background.

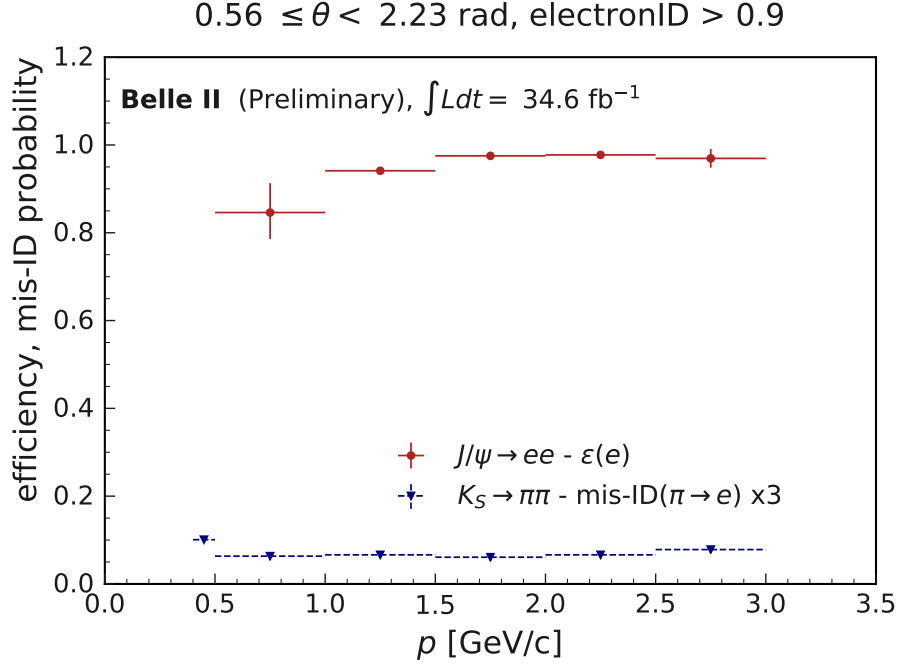


FIG. 8: J/ψ and K_S^0 efficiency and fake rate overlay for **electronID** integrated over the entire ECL barrel region, as a function of track momentum. Note that the hadron mis-identification rate has been inflated by a factor 3 for illustration purposes.

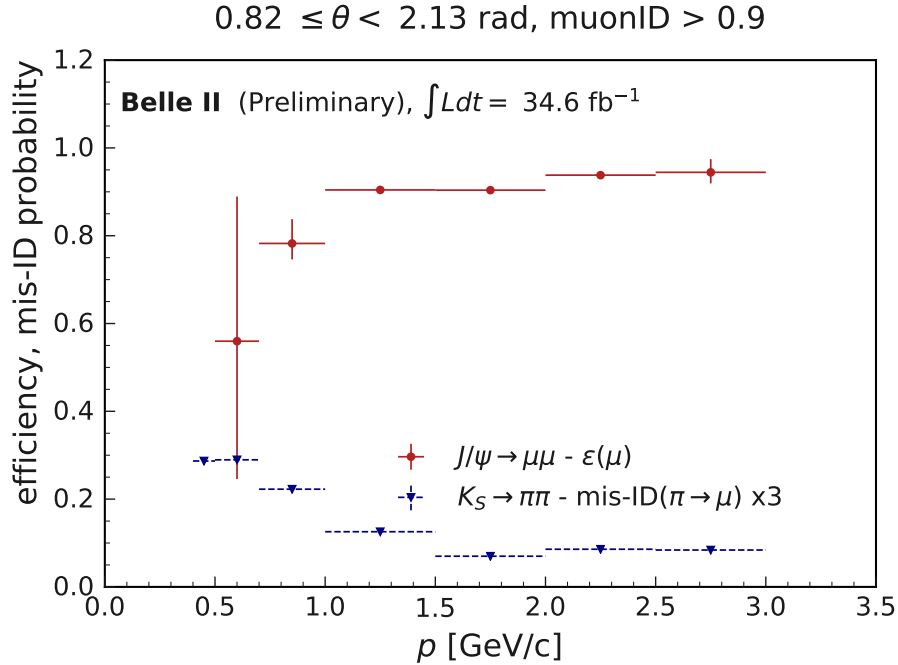


FIG. 9: J/ψ and K_S^0 efficiency and mis-identification rate overlay for **muonID** integrated over the entire KLM barrel region, as a function of track momentum. Note that the hadron mis-identification rate has been inflated by a factor 3 for illustration purposes.

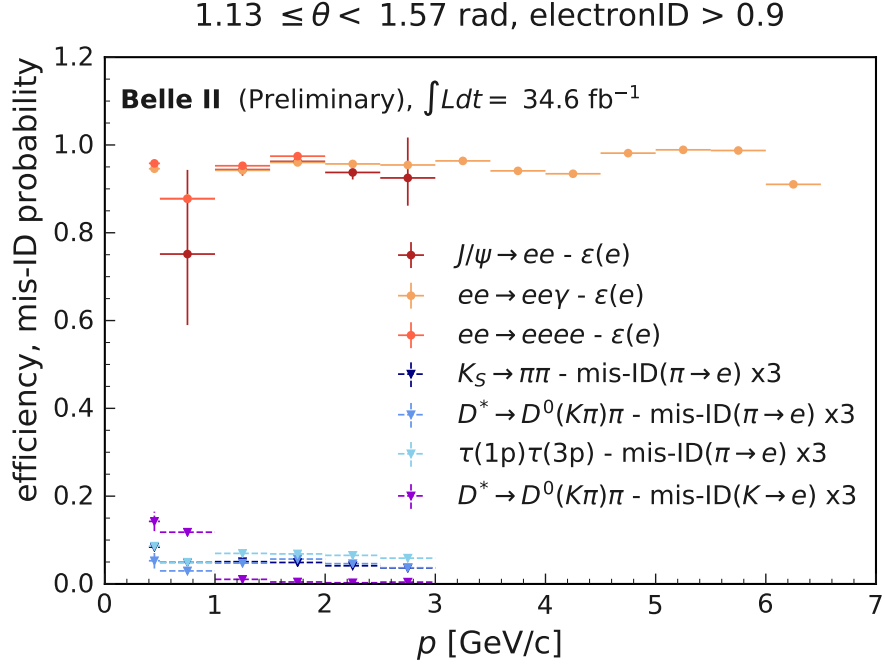


FIG. 10: Example ECL barrel bin for `electronID` with all measurements, efficiencies and hadron-lepton mis-identification rates overlaid. Note that the mis-identification rate has been inflated by a factor 3 for illustration purposes.

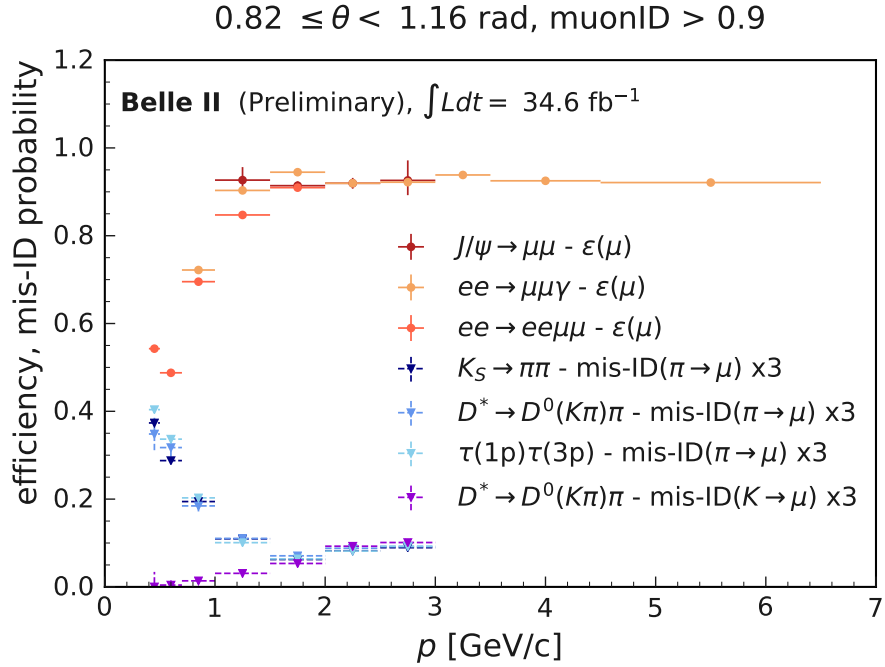


FIG. 11: Example KLM barrel bin for `muonID` with all measurements, efficiencies and hadron-lepton mis-identification rates overlaid. Note that the mis-identification rate has been inflated by a factor 3 for illustration purposes.